

## Reduction of detent force in flat Permanent Magnet Linear Synchronous Machines by means of three different methods

Martínez G., Atencia J., Martínez-Iturralde M., García Rico A., Flórez J.

Escuela Superior de Ingenieros (TECNUN). Universidad de Navarra  
 Paseo Manuel de Lardizábal 13, 20018 San Sebastián (SPAIN)  
 Tel.: +34 943 219877 Fax: +34 943 311442. E-mail: [gmartinez@tecnun.es](mailto:gmartinez@tecnun.es)

**Abstract** - This paper proposes two different techniques to reduce detent force in flat Permanent Magnet Linear Synchronous Motors (PMLSM). The first one is the choice of an optimal constructive design, taking into account the width and arrangement of the magnets, and the length and shape of the solid iron core. The second is the employ of a force compensator in the control algorithm, which counteracts the detent force effects.

Both methods are based on a Fourier analysis of the detent force curve as a function of the machine position. The curve is broken down into harmonics. The constructive method considers that each harmonic has its peculiar source and is independent from the others. The force compensator employs a detent force model based on the Fourier series of the curve.

The two methods were tested separately, and their results were compared. Experimental tests were performed to verify the effectiveness of the methods. A very important reduction with a constructive optimization of the machine was achieved. The reduction by means of a compensator in the control scheme also reaches excellent results. In order to achieve the maximum reduction of detent force, both techniques can be combined. This measure will increase the precision features of this kind of machines.

### I. INTRODUCTION

Linear electrical machines employed as linear actuators can be highly suitable in special industry applications, where the task requires a dynamic performance impossible to provide for rotary machines.

Among linear machines, Permanent Magnet Linear Synchronous Machines (PMLSM) have higher performance than other topologies, such as a bigger thrust/size ratio, more efficiency and faster response. However, PMLSMs present an important drawback due to the detent force characteristic of this kind of machines. Detent force is particularly troublesome when accurate positioning is needed or low constant speed is required. It depends on the position of the drive, and produces speed ripple, and consequently, tracking errors.

There are two main different ways of dealing with cogging (detent force), by an appropriate mechanical design, and by acting on the control system of the machine. A constructive optimization is based on the analysis of the physical sources of the problem, and counteracts the negative effects of detent force acting on the prototype geometry. On the other hand, the forces can be minimized with a suitable control algorithm including a force compensator [1].

Very important reductions of detent force have been achieved using each method alone [2]-[3]. Experimental tests were performed to verify the effectiveness of both

techniques. This paper shows a comparison of the results obtained from the separate implementation of both methods. Finally, the paper proposes the combination of both techniques in order to eliminate the negative effects of detent force and suppress completely the force and speed ripple.

### II. DESCRIPTION OF THE PROTOTYPE AND THE CONTROL STRATEGY

#### A. Prototype

The prototype is a Flat Permanent Magnet Linear Synchronous Motor. Fig. 1 shows its structure. The primary core is 50 mm wide, and the remaining physical dimensions are shown in Table I.

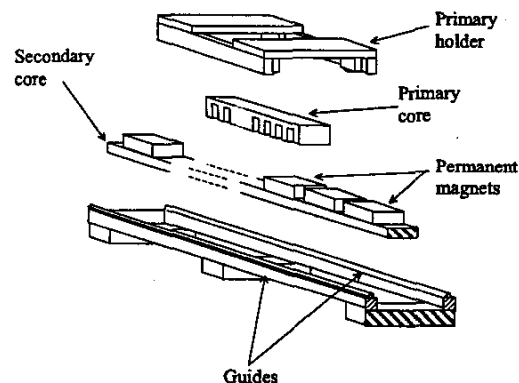


Fig. 1. Prototype structure

The secondary part is composed of permanent magnets placed on a secondary iron core. Rare earth magnets (SmCo) were employed, because of their high energy/volume ratio. The optimal width of the magnets was chosen to minimize the non-linearities in the production of force.

TABLE I  
 PROTOTYPE DIMENSIONS

PMLSM prototype		
Primary	type	three phase
	turns / coil	225
	armature material	iron
	pole pitch ( $\tau$ )	49.2 mm
	slot pitch ( $\tau_s$ )	16.4 mm
Secondary	material	rare earth magnets
	airgap (g)	5 mm
	height of magnets	7 mm
	width of magnets ( $\tau_m$ )	37 mm

### B. Control strategy

Field Oriented Control (FOC) was employed to control the machine. Fig. 2 shows the block diagram of the control algorithm used to test the performance of the machine.

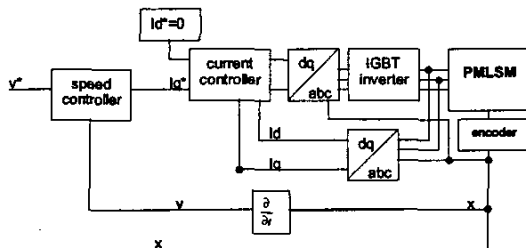


Fig. 2. Control block diagram

Vector control allows a good speed and position control, and is commonly used with permanent magnet actuators. Only the position of the machine and the current values must be known. The currents are measured with two current sensors, and the position of the drive is given by an encoder.

Every control loop works with PI controllers. The control algorithm has been implemented with a DSP controller board, whilst the power system consists in a three-phase IGBT inverter with a DC-bus voltage of 310 V. The PWM is performed at the switching frequency of 5 kHz.

### III. CONSTRUCTIVE OPTIMIZATION OF THE MACHINE

The detent force of the prototype was measured along a distance  $20\tau = 0.984$  m ( $\tau = 0.0492$  m = pole pitch). A force vs. displacement curve  $F = f(x)$  was obtained. Detent force depends on the position of the drive, and it was found that the curve is periodical with *period* =  $\tau$ . The curve was Fourier-analysed to determine its harmonics.

The technique proposed considers detent force as a superposition of independent cogging harmonics [2].

$$\begin{aligned}
 F_{detent} = & a_1 \sin\left(\frac{2\pi x}{\tau} + \varphi_1\right) + a_2 \sin\left(\frac{4\pi x}{\tau} + \varphi_2\right) + \dots \\
 & \dots + a_n \sin\left(\frac{2n\pi x}{\tau} + \varphi_n\right)
 \end{aligned} \quad (1)$$

Each harmonic of the curve has its peculiar source, and can be minimized acting on that peculiar source alone. It was found that detent force has two main harmonics: the first one due to the slots of the primary with period  $\tau_s$  (slot pitch), and the second one due to the length of the machine and its ends, with period  $\tau$ . It must be pointed out that  $\tau = 3\tau_s$ , so these two main harmonics are the first and the third ones, and the force curve can be estimated as follows:

$$F_{detent} = a_1 \sin\left(\frac{2\pi x}{\tau} + \varphi_1\right) + a_3 \sin\left(\frac{6\pi x}{\tau} + \varphi_3\right) \quad (2)$$

where the values of  $a_i$  and  $\varphi_i$  are taken from the Fourier analysis of the experimental force curve.

In order to reduce cogging force the following actions can be performed:

- Definition of the width of the magnets and their arrangement (skewing). That has a very important influence on the third harmonic amplitude  $a_3$ .
- Optimal choice of the primary iron core length and shape. That has influence on the first harmonic value  $a_1$ .

#### A. Width and arrangement of the permanent magnets

Several FEM simulations were performed to find the detent force values corresponding to different widths of the magnets. It can be empirically demonstrated that the optimal width for the permanent magnets  $\tau_b$  is:

$$\tau_b \propto \frac{3}{4}\tau \quad (3)$$

The permanent magnets of the prototype are 37 mm wide, and they were skewed a slot pitch in order to minimise the third harmonic [2] (Fig. 3).

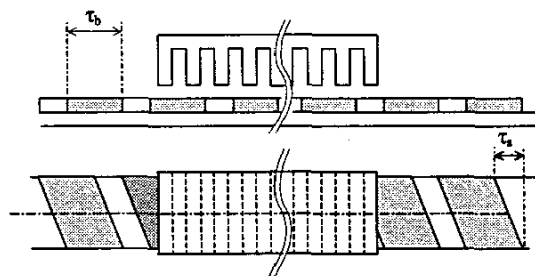


Fig. 3. Magnet skewing

#### B. Primary iron core length and shape

The ends of the linear machine are the main cause for the first harmonic of cogging [2]. Choosing an optimal distance between these ends, the forces can be cancelled. It was found that the optimal length for the primary core was:

$$l = \left(n - \frac{1}{2}\right)\tau \quad n = 1, 2, 3, \dots \quad (4)$$

Fig. 4 shows how the primary iron core was modified in order to reach its optimal length.

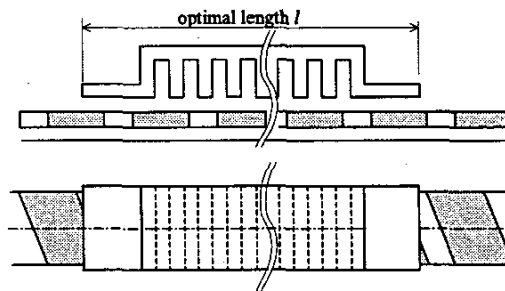


Fig. 4. Modification of the iron core length

The shape of the solid iron core has a hand in the first harmonic of the force. Skewing only the ends of the armature reduces its amplitude, and does not affect significantly the thrust that the linear machine can develop. Fig. 5 shows how the solid iron core was modified.

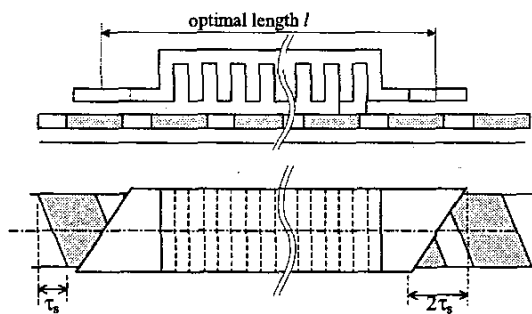


Fig. 5. Modification of the prototype geometry

The experimental tests showed excellent results. A very important reduction of cogging force was achieved, as seen in Fig. 6.

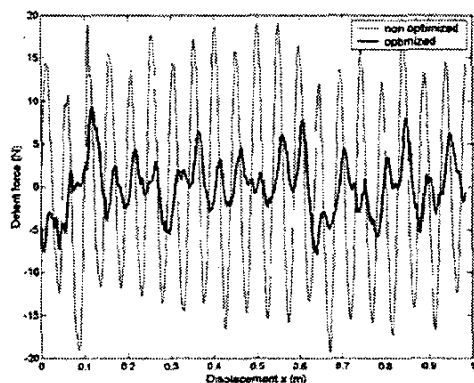


Fig. 6. Detent force as a function of displacement of the drive

The choice of the optimal length and shape for the solid iron primary core makes the detent force decrease by maximum values of 62.5 %.

#### IV. CONTROL ALGORITHM: RFOC WITH FORCE COMPENSATOR

Another way to reduce the effects of detent force and optimize the performance of the machine is to act on its control algorithm.

Fig. 7 shows the control scheme used to test the performance of the machine with detent force compensation. The algorithm includes a force compensator that achieves a reduction of the speed ripple generated by detent force.

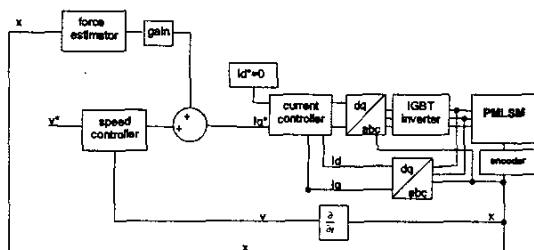


Fig. 7. Control block diagram with force compensator

Detent force can be expressed as shown in (1), and the two main harmonics are the first and the third ones. Neglecting the low amplitude harmonics, (4) shows the model used to calculate the detent force in the compensator.

$$F_{detent} = a_1 \sin\left(\frac{2\pi x}{\tau} + \varphi_1\right) + a_2 \sin\left(\frac{4\pi x}{\tau} + \varphi_2\right) + a_3 \sin\left(\frac{6\pi x}{\tau} + \varphi_3\right) \quad (5)$$

In this case, the second harmonic was taken into account, in order to improve the model accuracy.

In RFOC controlled PMLSMs, if the current  $i_d^*$  is set to zero, the whole flux of the machine is generated by the permanent magnets, and the thrust is generated by the current  $i_q$ .

$$F = \frac{3}{2} p \frac{\pi}{\tau} \Psi_F i_q = K i_q \quad (6)$$

where:

- $p$  = number of pole pairs
- $\tau$  = pole pitch
- $\Psi_F$  = excitation flux linkage

$\Psi_F$  is generated by the permanent magnets. In this case,  $\Psi_F$ ,  $p$  and  $\tau$  are constant values, so the thrust is directly proportional to  $i_q$ .

With the force compensator shown in Fig. 7, the current reference command  $i_q^*$ , and therefore, the thrust developed by the machine has two components: the first one is generated by the current  $i_q^*$  necessary to reach the speed reference command in absence of detent force, and the second one is generated by the current  $i_q^*$  necessary to counteract the detent force.

The validity of the model can be realized in Fig. 8, where the calculated force curve fits the measured one. The figure corresponds to the prototype with the optimal width and arrangement of the magnets, but without any constructive optimization of the iron core.

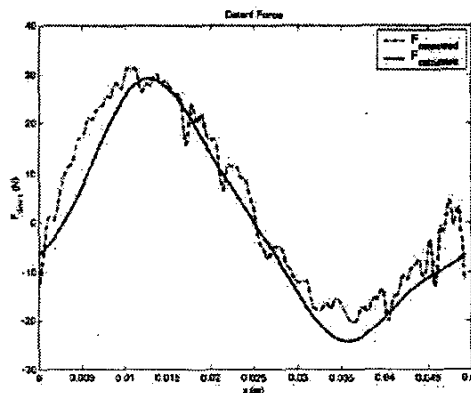


Fig. 8. Detent force measured and calculated along a pole pitch  $\tau$

The optimized prototype presents different values of detent force. Its force curve has lower values and is more irregular. However, the same model can be used, but with different values  $a_i$  and  $\varphi_i$ . Fig. 9 shows how the calculated force curve fits the measured one.

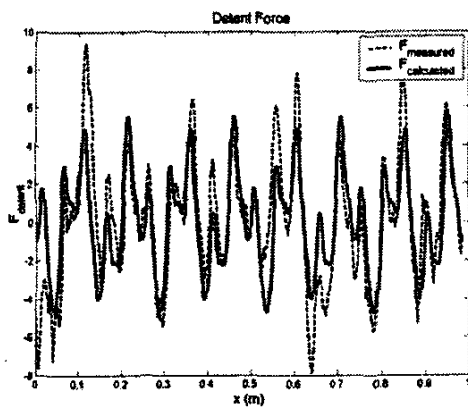
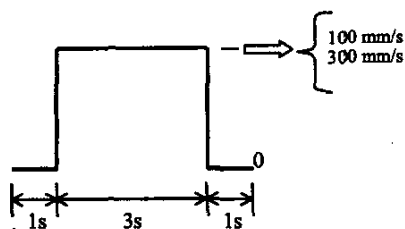


Fig. 9. Detent force measured and calculated along 20t

### V. EXPERIMENTAL TESTS

The prototype was tested in order to characterise and compare the constructive optimization and the force compensator efficiencies. The speed, precision and current consumption were analysed. The purpose of the analysis is to verify the effectiveness of the two techniques, quantify the reduction of force and speed ripple, and determine the suitability of the different ripple reduction methods depending on the applications.

Speed tests were carried out, using the reference commands shown in Fig. 10. The results of speed tests with 0.1 and 0.3 m/s step reference commands are presented.



Speed step command

Fig. 10. Reference command

### VI. RESULTS

#### A. Constructive design

Fig. 11 and Fig. 12 show the speed response of the prototype under step commands of 0.1 and 0.3 m/s respectively. The reference command ( $v^*$ ), the response of the original prototype ( $v_{nop}$  - non optimized -), and the response of the optimized prototype ( $v_{op}$ ) are presented.

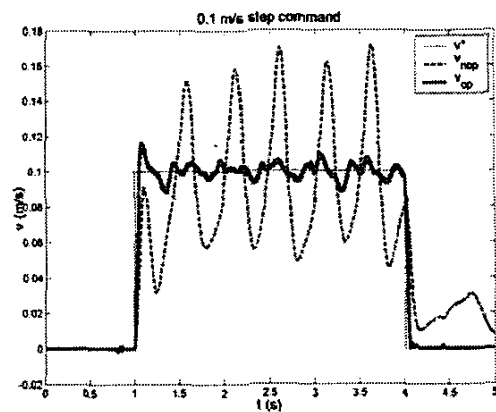


Fig. 11. Speed response with 0.1 m/s reference command

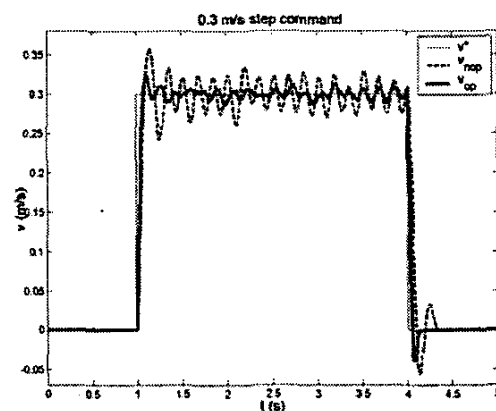


Fig. 12. Speed response with 0.3 m/s reference command

At low and moderate speeds, the speed ripple reduction is very significant. The constructive optimization of the machines achieves a detent force reduction of 86 %.

#### B. Vector control and force compensation

Fig. 13 and Fig. 14 show the speed response of the non-optimized prototype under step commands of 0.1 and 0.3 m/s respectively. The reference command ( $v^*$ ), the response without force compensation ( $v_{nc}$ ), and the response with force compensation ( $v_c$ ) are presented.

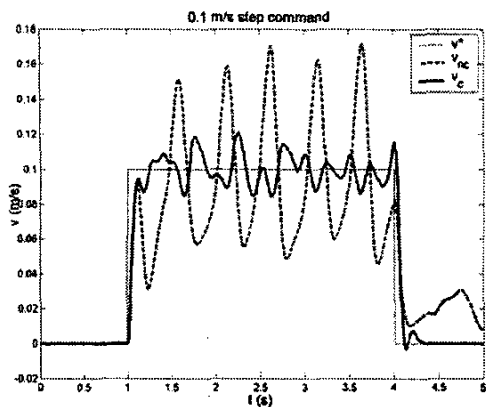


Fig. 13. Speed response with 0.1 m/s reference command

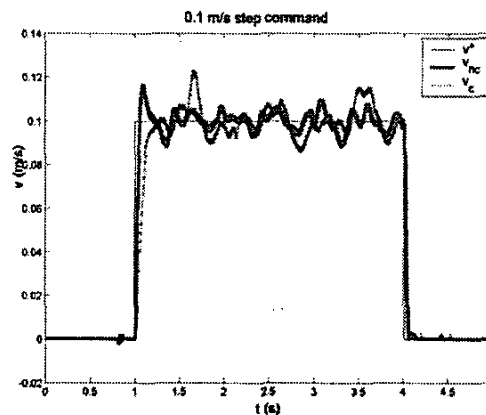


Fig. 15. Speed response with 0.1 m/s reference command

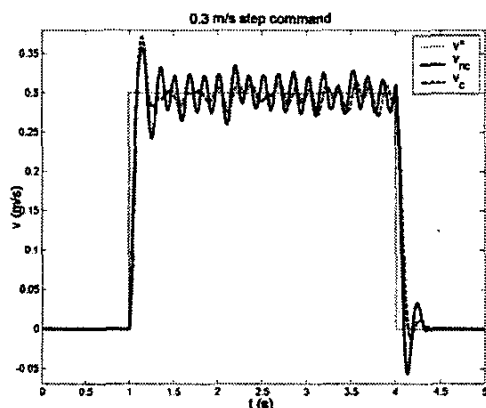


Fig. 14. Speed response with 0.3 m/s reference command

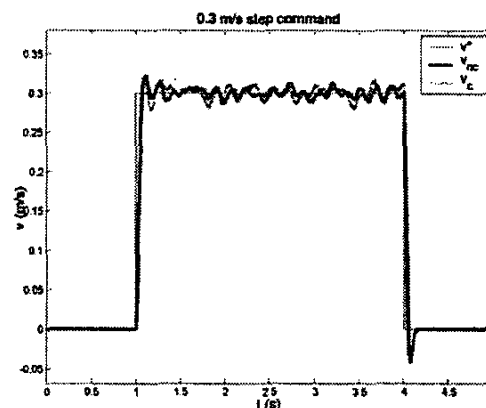


Fig. 16. Speed response with 0.3 m/s reference command

A very important reduction of the speed ripple is reached. In case of 0.3 m/s response a maximum reduction of 74 % was achieved for the speed error. For the 0.1 m/s response, this percentage increases to 91 %.

*C. Optimized design and force compensator working simultaneously*

Fig. 15 and Fig. 16 show the speed response of the optimized prototype under step commands of 0.1 and 0.3 m/s respectively. As in previous cases, the reference command ( $v^*$ ), the response without force compensation ( $v_{nc}$ ), and the response with force compensation ( $v_c$ ) are presented.

By looking at Fig. 15 and Fig. 16 it can be noticed that the speed error decreases achieved are much less significant than in previous cases.

Finally, Fig. 17 and Fig. 18 summarize the results of the tests, showing the four speed responses corresponding to each step reference command.

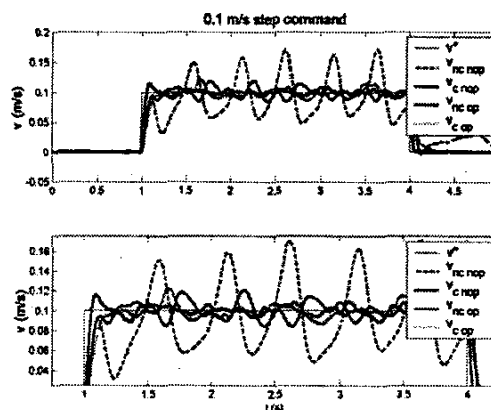


Fig. 17. Speed response with 0.1 m/s reference command

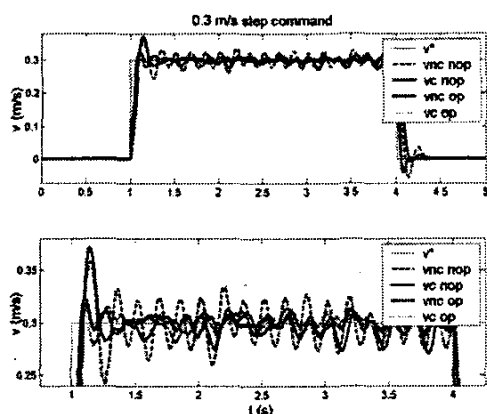


Fig. 18. Speed response with 0.3 m/s reference command

Table II summarizes the force and speed error decreases reached with both methods of reducing cogging force, each method working alone.

**TABLE II**  
FORCE AND SPEED RIPPLE DECREASES

Constructive actions		Control algorithm	
Force reduction		Speed error reduction	
Skewing the magnets	23.43 %	0.1 m/s	91 %
Optimal core length	48.54 %	0.3 m/s	74 %
Optimal core shape	86 %		

## VII. CONCLUSIONS

Two different techniques to minimize the effects of detent force in PMLSMs are presented. Each method has advantages and drawbacks. Experimental tests were performed to verify the effectiveness of both techniques.

Depending on the application a machine will be used for, and considering constructive and economic aspects, one of the two ways to compensate detent force must be chosen.

Applying the developed control algorithm to a prototype with a specific constructive design to reduce detent force, the force and speed ripple can be almost completely eliminated, theoretically. The detent force model of the optimized prototype was developed. The validity of the model was analysed. The calculated force curve fits satisfactorily the measured one, but the force values reached with the optimal constructive design are very low, and under these conditions, the force compensator does not affect the performance of the machine significantly.

As a summary of the developed analysis, it can be pointed out:

- An optimal constructive design of the prototype can reach excellent results reducing the negative effects of detent force. The force ripple can be reduced by 86 % or more, and that will improve significantly the precision features of the machine.
- At low and moderate speed, the force compensator has an important influence on the speed ripple. The maximum values of speed error can be reduced by 91 %.

The control algorithm with force compensator will improve the precision features of the machine and reduce tracking errors.

- The force compensator acting on a constructively optimized prototype affects less significantly to the machine performance. In this case the detent force values are very low and the difficulty to notice the improvement of the speed ripple increases.
- Depending on the application a PMLSM will be used for, the tasks will require different levels of accuracy. Two different ways (design and control) to reduce detent force were proposed, and their efficiency was verified. Considering constructive and economic aspects, and taking into account the precision level demanded by the applications, the best way to compensate detent force must be chosen: the constructive optimization, the force compensator, or both methods working simultaneously.

## REFERENCES

- [1] G. Otten, J.A. deVries, J. van Amerongen, A.M. Rankers, E.W. Gaal, "Linear Motor Control Using a Learning Feedforward Controller", IEEE Trans. On Mechatronics, vol. 2, n° 3, pp. 179 – 187, September 1997.
- [2] J. Atencia, G. Martínez, A. García Rico, J. Flórez, "Minimization of cogging force in flat Permanent Magnet Linear Motors", Proceedings of the LDIA Conference, Nagano (Japan), 17-19 October 2001.
- [3] G. Martínez, J. Atencia, A. García Rico, J. Flórez, "Vector control of Permanent Magnet Linear Synchronous Machines with detent force compensation", Proceedings of the MED Power 2002 Conference, Athens, November 2002.
- [4] T.M. Jahns, W.J. Soong, "Pulsating Torque Minimization Techniques for Permanent Magnet AC Motor Drives – A review", IEEE Trans. on Industrial Electronics, vol. 43, n° 2, pp. 321 – 326, April 1996.
- [5] T. Yoshimura, H.J. Kim, M. Watada, S. Torii, D. Ebibhara, "Analysis of the reduction of detent force in a permanent magnet linear synchronous motor", IEEE Trans. on Magnetics, vol. 31, n° 6, pp. 3728 – 3730, November 1995.